Universidad de Cantabria

Departamento de Física Moderna

CSIC - Universidad de Cantabria

Instituto de Física de Cantabria

Detection of Point Sources in Maps of the Cosmic Microwave Background Radiation by means of Optimal Filters

A dissertation submited in partial of the requirements

for the degree of Doctor of Philosophy in Physics

by

Marcos López-Caniego Alcarria

2006

CHAPTER 5

Linear and Quadratic Fusion of Images

This chapter considers the linear and quadratic fusion of a set of n-dimensional images. We aim to produce a single image that amplifies the signal and minimizes the noise. As a starting point, we consider wavelet subimages of a single image. We use three wavelets, the *Mexican Hat Wavelet Family (MHWF)* and the undecimated multiscale method to obtain 3N subimages. As an application we consider the detection of galaxies in Cosmic Microwave Background radiation maps. We use linear and quadratic fusion to produce a combined image for the detection. Moreover, we test these ideas for the simple case of point sources embedded in white noise and for the case of realistic simulations of microwave images for the 44 GHz channel of ESA's Planck satellite. In the last case, using quadratic fusion and allowing $\simeq 1\%(5\%)$ of false alarms we detect $26\%(23\%)$ more sources than using linear fusion at the $5\sigma(4\sigma)$ level, see López-Caniego et al. [89].

5.1 Introduction

One of the main challenges in the analysis of n-dimensional images is to overcome the problem of separating a localized signal from a background. In some cases the signal can be modeled by a set of sources with spherical symmetry that are diluted in the background. An interesting case corresponds to sources whose profile can be approximately described by a Gaussian function. An example is given in astrophysics/cosmology by a point source observed with an antenna with a Gaussian response. For exam-

ple, in microwave Astronomy the sky is filled with radiation coming from the Cosmic Microwave Background (CMB), that is a remnant of the Big Bang which carries very valuable information about the primitive conditions of the Universe, plus diffuse emissions due to the Galaxy (Galactic dust, synchrotron and bremsstrahlung emission) and emission due to clusters of galaxies. Embedded in this background it is possible to observe galaxies, that due to the low angular resolution of microwave experiments appear as "points" convolved with the (approximately Gaussian) response of the detectors. Therefore they are usually referred to as *point sources* (PS) in the astrophysicists' jargon.

Fusion or combination of images (Maitre et al. [95], Wang et al. [150] can help to enhance the signal (in our case, the point sources in CMB maps) with respect to a noisy background. Let us consider different images and/or images at different frequencies corresponding to the same object. A relevant problem is how to fuse these images in order to get the *best* single image to be analysed. There are different ways to combine the images: pixel level (Blum [13]), block level (Li et al. [92]) and image decomposition (Bijaoui et al. [12], Piella [112]). Another aspect is related to the rule assumed to combine these data: linear, non-linear (Schrater [126]).

Another interesting case is the fusion of subimages obtained from a single image. Let us imagine we decompose an image into different subimages (e.g. using wavelet analysis). The question is how to combine such subimages in order to optimize the separation of the sources. This case has not been considered in the literature as far as we know. We would like to remark that the *fusion* of images or subimages regarding feature detection is the first step to generate the *best* image to be analysed. Afterwards, one needs to apply a detector to mark out the features. In astrophysics/cosmology it is standard to consider thresholding above the 5σ level, where σ is the dispersion of the image, as a simple linear detector.

After the introduction of the framework for *quadratic fusion* of images, we apply it to the fusion of subimages obtained applying the *Mexican Hat Wavelet Family (MHWF)* with the undecimated multiscale technique. This family has been recently introduced (González-Nuevo et al. [51]). We test the method with two types of images: (i) distribution of sources on a white noise background and (ii) distribution of sources on a color noise background typical of a microwave observation of the sky.

The overview of this work is as follows: in section 5.2 we describe the method for combining a set of n-dimensional images using a linear and a quadratic approach. In section 5.3 we present a scheme to produce the subimages needed for the fusion, the MHWF and the undecimated multiscale method. For comparison, we review a com-

mon approach in Astronomy that is to use the Mexican hat wavelet to filter out the background in order to enhance the point sources. In section 5.4 we apply these techniques to the interesting case of detecting point sources embedded in white noise and for the more realistic case of color noise (CMB maps). Finally, in section 5.5 we summarise our results.

5.2 Linear and quadratic fusion

Let $d^i(\vec{x})$ be N images in n-dimensional space ($i = 1, \ldots, N$, $\vec{x} \in \Re^n$). Consider that these images are the superposition of a signal $s^i(\vec{x})$ and noise $n^i(\vec{x})$. We will assume that the signal is a set of point sources characterised by their amplitude A and profile $\tau^i(\vec{x} - \vec{x_a})$, where $\vec{x_a}$ is the position of the source and the sources have a small contribution to the total power of the image. The background $n^i(\vec{x})$ is modeled by random fields with the following properties at any point $\vec{x}$

$$\langle n^i \rangle = 0, \quad \langle n^i n^j \rangle = C^{ij} = C^{ji}, \tag{5.2.1}$$

$$\begin{aligned} \langle n^i n^j n^k \rangle &= 0, \\ \langle n^i n^j n^k n^l \rangle &= C^{ij}C^{kl} + C^{ik}C^{jl} + C^{il}C^{jk}, \end{aligned} \tag{5.2.2}$$

where $\langle\rangle$ means mean value either on the image or in the sense of realizations of the field. Note that if the backgrounds of the images are Gaussian, then condition (5.2.2) is satisfied. Let us focus on a concrete compact source at the origin ($\vec{x_a} = \vec{0}$) being represented by

$$s^i(\vec{x}) = A\tau^i(\vec{x}), \quad \tau^i \equiv \tau^i(\vec{0}), \tag{5.2.3}$$

where A is the amplitude and τ the profile.

5.2.1 Linear Fusion

In this case we only need to assume the condition (5.2.1) given above that involves mean value and the correlation between the images at the same point for the noise. We define the *linear fusion* d_L of the N images as the linear superposition

$$d_L(\vec{x}) = \sum_i a_i d^i(\vec{x}), \tag{5.2.4}$$

where a_i are constants.

Now, we are going to express the conditions to obtain a combination such that

a) $\langle d_L(\vec{0})\rangle = A$, i. e. $d_L(\vec{0})$ is an *unbiased* estimator of the amplitude of the source,

b) The variance of d_L has a minimum, i. e. it is an *efficient* estimator.

With these conditions the problem is reduced to the minimization of σ_L^2 with respect to a_i, subject to a constraint $(a_i\tau^i = 1)$. Therefore, we get the best signal to noise ratio of the sources that is attainable with a linear combination of the images. The a_i that satisfy these conditions are given in matrix form by

$$a = \lambda C^{-1}\tau, \quad \lambda \equiv \frac{1}{\tau^t C^{-1}\tau}, \tag{5.2.5}$$

where we have introduced the column vectors $a \equiv (a^i)$ and $\tau \equiv (\tau^i)$ (τ^t is the transpose matrix) and the symmetric matrix $C \equiv (C_{ij}), C = C^t$. Taking into account the equation (5.2.4), the *fusion field* d_L can be written in a matrix form as

$$d_L = a^t d, \quad a \equiv \frac{C^{-1}\tau}{\tau^t C^{-1}\tau}, \tag{5.2.6}$$

and the *normalised amplitude* at the source position is

$$\nu_L \equiv \frac{\langle d_L\rangle}{\sigma_L} = AT^{1/2}, \quad T \equiv \tau^t C^{-1}\tau. \tag{5.2.7}$$

ν_L (or equivalently, the variance) will be considered as the performance measure when comparing different fission schemes. Notice that we are not considering an MMSE estimation because we are trying to detect point sources without any prior knowledge of their position and amplitude.

5.2.2 Quadratic Fusion

In this case we need to assume the conditions given by equations (5.2.1) and (5.2.2) that involve mean value and the correlations, up to 4th-order, between the images at the same point for the noise. We define the *quadratic fusion* d_Q of the N images as the linear plus quadratic superposition

$$d_Q(\vec{x}) = \sum_i a_i d^i(\vec{x}) + \sum_{i,j} b_{ij} d^i(\vec{x}) d^j(\vec{x}), \tag{5.2.8}$$

where a_i, b_{ij} are constants. The conditions to obtain a combination that optimizes the detection of the source in an analogous way as in the case of *linear fusion* are

a) $\langle d_Q(\vec{0})\rangle = \alpha A + \beta A^2$, i. e. $d_Q(\vec{0})$ is a quadratic estimator of the amplitude of the source (α and β are two free parameters),

b) The variance of d_Q has a minimum, i. e. it is an *efficient* estimator.

Therefore, the problem is reduced to the parameter minimization (with respect to a_i and b_{ij}) of σ_Q^2 with two constraints ($a_i\tau^i = \alpha$ and $b_{ij}\tau^i\tau^j = \epsilon$). The result is given in matrix form

$$a = \lambda C^{-1}\tau, \;\; \lambda \equiv \frac{\alpha}{\tau^t C^{-1}\tau}, \;\; b = \mu C^{-1}\Sigma C^{-1},$$
$$\Sigma \equiv \tau\tau^t, \;\; \mu \equiv \frac{\beta}{\left(\tau^t C^{-1}\tau\right)^2}, \tag{5.2.9}$$

where we have introduced the column vectors $a \equiv (a^i)$ and $\tau \equiv (\tau^i)$ and the symmetric matrices $C \equiv (C_{ij})$, $C = C^t$, $b \equiv (b_{ij})$, $b = b^t$. Taking into account the equation (5.2.8), the *fusion field* d_Q can be written in a matrix form as

$$d_Q = a^t d + d^t b d = \alpha p^t d + \beta (p^t d)^2, \quad p \equiv \frac{C^{-1}\tau}{\tau^t C^{-1}\tau}, \tag{5.2.10}$$

that is, necessarily the quadratic term must be proportional to the square of the linear one. Notice that the non-appearance of the cross quadratic terms is due to the assumption given by equation (5.2.2). Thus, the *quadratic fusion* is easy to implement by performing the linear combination d_L and adding a term that is proportional to the square of d_L, $d_Q = d_L + \epsilon d_L^2$ (we can always take $\alpha = 1$ if the linear term is present). The *normalised amplitude* at the source position is

$$\nu_Q \equiv \frac{\langle d_Q \rangle}{\sigma_Q} = AT^{1/2}\frac{1 + \epsilon A^2}{\left(1 + 2\epsilon^2 T^{-1}\right)^{1/2}},$$
$$\epsilon \equiv \frac{\beta}{\alpha}, \quad T \equiv \tau^t C^{-1}\tau. \tag{5.2.11}$$

ν_Q will be considered as the performance measure when comparing different fusion schemes. It is interesting to define the gains with respect to the *linear fusion*

$$\frac{\nu_Q}{\nu_L} = \frac{1 + \nu_L x}{\left(1 + 2x^2\right)^{1/2}}, \quad x \equiv \epsilon T^{-1/2}. \tag{5.2.12}$$

For the case of a "pure" *quadratic fusion* with $\alpha \equiv 0$, that is, a fusion without linear terms, we have

$$\frac{\nu_{Q(\alpha=0)}}{\nu_L} = 2^{-1/2}\nu_L. \tag{5.2.13}$$

Taking into account the last equations, one clearly obtains that a *quadratic fusion* is better than the linear one if $\nu_L > 2^{1/2}$. The maximum value of the gain is obtained for

$$\epsilon_{max} = T^{1/2}\frac{\nu_L}{2}, \quad \left(\frac{\nu_Q}{\nu_L}\right)_{max} = \left(1 + \frac{\nu_L^2}{2}\right)^{1/2}. \tag{5.2.14}$$

It is clear that for $\nu_L \gg 1$ the previous equation leads to $(\nu_Q/\nu_L)_{max} \simeq 2^{-1/2}\nu_L$ which is given by the "pure" quadratic term.

5.3 The Mexican Hat Wavelet Family

When we apply wavelets in $\Re^n$, we are decomposing a function on a basis that incorporates the local and scaling behaviour of the function. Therefore, the continuous transform involves translations and dilations

$$\Psi(\vec{x};\vec{b},R) \equiv \frac{1}{R^n}\psi\left(\frac{|\vec{x}-\vec{b}|}{R}\right), \tag{5.3.1}$$

where Ψ is the mother wavelet, R is the dilation scale and $\vec{b}$ is the translation. Then, the wavelet coefficient is defined as

$$w(\vec{b},R) = \int d\vec{x}\, f(\vec{x})\Psi(\vec{x};\vec{b},R), \tag{5.3.2}$$

$$w(\vec{b},R) = \int d\vec{q}\, e^{-i\vec{q}\vec{b}} f(\vec{q})\psi(qR),\ q \equiv |\vec{q}|, \tag{5.3.3}$$

in real and Fourier space, respectively.

We are interested in the problem of point source detection in the context of astronomical images. These objects appear as points in the sky at microwave frequencies, although in the images they are convolved with the beam of the instrument used for the observation. This beam can be approximated by a Gaussian and therefore we will concentrate on Gaussian profiles for our sources. We are going to introduce a new family of wavelets that can be derived from the Gaussian function using an undecimated multiscale method (González-Nuevo et al. [51]) and compare its performance with the Mexican hat wavelet (MHW) that has been recently used as a filter to detect point sources (e.g. Cayón et al. [19], Vielva et al. [144]).

5.3.1 The MHW as a filter

The MHW is defined to be proportional to the Laplacian of the Gaussian function, in two dimensions

$$\psi_{MH}(x) = \frac{1}{2\pi}(2-x^2)e^{-\frac{1}{2}x^2},\ \ x \equiv |\vec{x}|, \tag{5.3.4}$$

$$\psi_{MH}(q) = \frac{q^2}{2}e^{-\frac{1}{2}q^2}, \tag{5.3.5}$$

in real and Fourier space, respectively. Taking into account equation (5.3.3) and the Gaussian profile of the source in Fourier space $\tau(q) = \gamma^2\exp(-(q\gamma)^2/2)$, the expression of the wavelet coefficient for a Gaussian source filtered with the MHW at the scale R_n is

$$\frac{w}{T_0} = \frac{y^2}{(1+y^2)^2},\ \ y \equiv \frac{R_n}{\gamma}, \tag{5.3.6}$$

where T_0 is the amplitude of the source and γ is the beam width (i.e. the width of the profile).

5.3.2 The MHWF and the undecimated multiscale method

We can generalize the MHW on the plane and obtain three isotropic filters for which the distance is the natural scale variable to be dilated at any point (González-Nuevo et al. [51]). The first two filters, ψ_{vh} and ψ_d, are given by the first and second order Laplacian of the Gaussian filter. The first one is the usual MHW and the second one is referred to as *"diagonal Mexican hat wavelet"* (DMHW). The third one, ψ_c, is called the *"complementary Mexican hat wavelet"* (CMHW) and is such that we have a perfect reconstruction of any function in $\Re^2$ at any scale. Furthermore, we use the Gaussian filter as scaling function at any scale. This way we introduce a non-orthogonal, overcomplete basis. These functions are given in polar coordinates (x, θ) for any fixed and arbitrary point on $\Re^2$ by

$$\begin{aligned}
\varphi(x) &= \frac{1}{2\pi} e^{-\frac{x^2}{2}}, \\
\psi_{vh}(x) &= \frac{1}{2\pi} \left(1 - \frac{x^2}{2}\right) e^{-\frac{x^2}{2}}, \\
\psi_d(x) &= \frac{1}{2\pi} \left(1 - x^2 + \frac{x^4}{8}\right) e^{-\frac{x^2}{2}}, \\
\psi_c(x) &= \delta(\vec{x}) - \frac{1}{2\pi} \left(3 - \frac{3x^2}{2} + \frac{x^4}{8}\right) e^{-\frac{x^2}{2}},
\end{aligned} \tag{5.3.7}$$

where $\delta(\vec{x})$ is the 2D Dirac distribution. Their Fourier transforms are

$$\begin{aligned}
\varphi(q) &= e^{-\frac{q^2}{2}}, \\
\psi_{vh}(q) &= \frac{q^2}{2} e^{-\frac{q^2}{2}}, \\
\psi_d(q) &= \frac{q^4}{8} e^{-\frac{q^2}{2}}, \\
\psi_c(q) &= 1 - \left(1 + \frac{q^2}{2} + \frac{q^4}{8}\right) e^{-\frac{q^2}{2}},
\end{aligned} \tag{5.3.8}$$

and these functions have the following behaviour when $q \to 0$

$$\varphi(q) \to 1,\ \Psi_{vh}(q) \to q^2,\ \Psi_d(q) \to q^4,\ \Psi_c(q) \to q^6. \tag{5.3.9}$$

We remark that the CMHW allows one to have perfect reconstruction, and is defined as the Dirac delta minus the other three functions (Gaussian + MHW + DMHW). We also notice that the convolution of the image with Ψ_{vh} and Ψ_d are equivalent to study the 2nd and 4th-order invariant differences of the image filtered with a Gaussian, assuming the appropriate boundary conditions.

The undecimated multiscale method (González-Nuevo et al. [51]) is a pyramidal method that allows one to decompose any image $f(\vec{q})$ at any scale (multiscale analysis), using

the analysing wavelets ψ_{vh}, ψ_d and ψ_c. In particular, for a pixelized image with pixel size l_p, we filter the image at this scale $R_1 = l_p$ and the image is decomposed, in Fourier space, as follows

$$\begin{aligned} f(\vec{q}) &= w_{vh}(R_1) + w_d(R_1) + w_c(R_1) + w_s(R_1), \\ w_{vh}(R_1) &= \psi_{vh}(qR_1)f(\vec{q}), \;\; w_d(R_1) = \psi_d(qR_1)f(\vec{q}), \\ w_c(R_1) &= \psi_c(qR_1)f(\vec{q}), \;\; w_s(R_1) = \varphi(qR_1)f(\vec{q}), \end{aligned} \tag{5.3.10}$$

where $w_s(R_1)$ is the approximation image. Then we apply the wavelet family at the scale $R_2 = 2l_p$ to the approximation image $w_s(R_1)$, and continue the scheme until the scale R_n. Therefore, the image $f(\vec{q})$ can be analysed and decomposed in different scales nl_p

$$f(\vec{q}) = \sum_i [w_{vh}(R_i) + w_d(R_i) + w_c(R_i)] + w_s(R_n) \tag{5.3.11}$$

The undecimated method has two very interesting characteristics: i) it is a multiscale approach that allows to study different resolution levels of the image, ii) the family of wavelets is isotropic.

5.4 Detection of point sources

The aim of this work is to improve the detection of point sources. In figure 5.1 we show a schematic representation of the procedure that we follow. We make two sets of simulations. In the first case, we simulate point sources convolved with a Gaussian beam to which we add white noise. In the case of Planck simulations, we simulate CMB and Galactic foregrounds plus point sources, we convolve the image with a Gaussian beam to model the response of the instrument (FWHM=24 arcmin) and then add white noise. Then we decompose the image into subimages, using three wavelets at different scales. Following the *quadratic fusion* technique proposed in section 5.2, we combine them and apply a simple detection criterion. The images are 118×118 pixels in size (6 arcmin per pixel) and the CPU time needed to generate and completely study every realization is of the order of one minute in a P4 computer.

5.4.1 White Noise

We have simulated 1000 realizations of the background noise with a flat power spectrum and added a Poisson distribution of point sources following González-Nuevo et al. [50], Toffolatti et al. [141]. This model is in good agreement with the most recent observations at these frequencies. The sources are randomly distributed in the image with

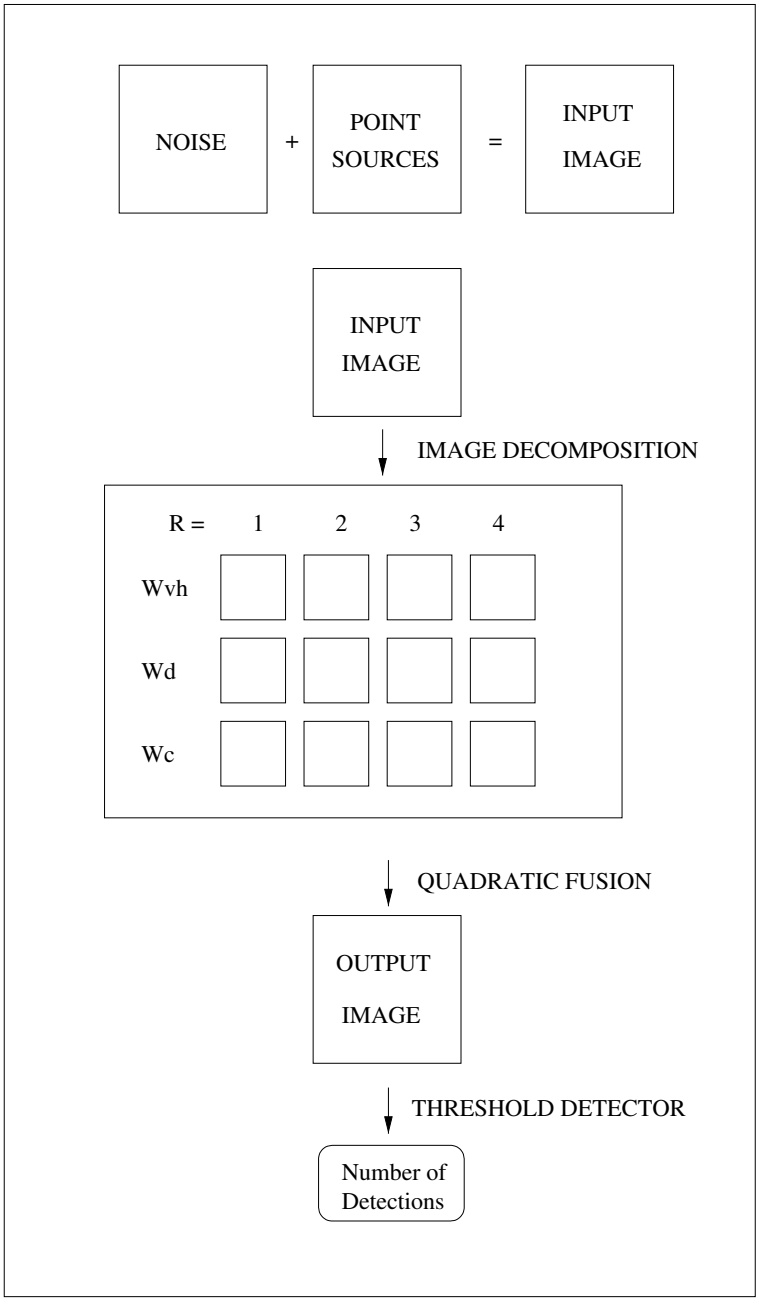

Figure 5.1 Schematic representation of the followed process. First, generate the input image with a background noise plus a signal (point sources). Second, decomposition into 12 subimages with the three wavelets Ψ_{vh}, Ψ_d and Ψ_c at six different scales R. Third, combination of these subimages and simple threshold detector application.

amplitudes following approximately a power-law distribution ($dN/dA \propto A^{-2.7}, A \geq 100mJy$) and the average $< S/N > \approx 4.9$. Then we have decomposed every one of these images into 12 subimages by means of the MHWF and the undecimated multiscale method. We have used the three wavelets from the MHWF for 4 different scales $R = \{1, 2, 3, 4\}$ in pixel units. We choose these scales because are the ones closer to the one associated to the FWHM of the sources ($R_s \simeq 2$ in pixel units). Considering the *linear* and *quadratic fusion* techniques we combine the 12 subimages into one with minimum variance. In particular, we consider the linearly fusioned image as well as several cases for the quadratic fusion for different values of ϵ. We apply a simple thresholding detector to the original image, that is, we count objects that are above a certain threshold, e.g. 5 times the dispersion of the image (5σ thresholding). This is the standard approach in astronomical data analysis. Then, we average together the number of detected objects for the 1000 simulated fields. We know the distribution of sources that we have added to every noise realization and compare the list of detected candidates with the list of actual sources. This allows us to give the exact number of detections or false alarms (spurious detections) above 5σ, if any. Furthermore we can calculate the average gain with respect to the original image for all the detected sources.

The results for these simulations are shown in Table 5.1, where N_{det} denotes the average number of real detections and N_f the average number of false alarms (or spurious detections). We compare the linear case with three quadratic cases with $\epsilon = (5000, 8000, 25000)$. For comparison purposes we have included in the previous table the number of real and false alarms obtained filtering the input image with the well known standard Mexican hat wavelet at the optimal scale (MHWopt, Vielva et al. [144]). The MHWopt is the standard Mexican hat wavelet with a scale parameter R_{opt} such that the signal to noise of the source with respect to the filtered background is maximum. For the case we are considering $R_{opt} = 2.9$ in pixel units.

For the linear case, we find that the average number of real detections N_{det} is 5.48, the average number of false alarms N_f is 0.003 and the ratio between them is $r = 0.05\%$. If we compare this case with the MHWopt, with $N_{det} = 4.19$ (and $r \simeq 0$), the improvement is $\simeq 23\%$. Regarding the *quadratic fusion*, we have exhaustively explored the parameter ϵ in the range $0 - 25000$. In the different tables, we give the results only for a few illustrative values of ϵ in order to compare -with similar ratios- with the linear and the MHWopt.

We perform a similar analysis comparing the MHWopt and the *quadratic* case, with $r \simeq 0.05\%$ and $r = 0$, respectively. The average number of detections are 4.19 (for the MHWopt) and 5.60 (for $\epsilon = 8000$), which implies a 25% improvement. We remark that

5σ	*Real*	*MHW*	*Linear*	*Quadratic*		
ϵ	-	-	0	5000	8000	25000
N_{det}	4.100	4.190	5.480	5.540	5.600	5.670
N_f	0.007	0	0.003	0.003	0.003	0.009
$r(\%)$	0.17	0	0.05	0.05	0.05	0.15
$< G >$	1.0	1.6	2.0	4.3	4.6	5.1

Table 5.1 5σ detections for white noise + PS. N_{det} denotes the average number of real detections, N_f the average number of false alarms, $r \equiv 100 \times N_f/(N_{det} + N_f)$. $\langle G \rangle \equiv \frac{\nu}{\nu_{or}}$ is the average gain of the detected sources with respect to the original image

4σ	*Real*	*MHW*	*Linear*	*Quadratic*		
ϵ	-	-	0	2000	5000	8000
N_{det}	6.550	5.650	7.705	7.540	7.480	7.470
N_f	0.024	0	0.006	0.010	0.014	0.020
$r(\%)$	0.36	0	0.08	0.13	0.2	0.3
$< G >$	1.0	1.6	2.0	5.0	5.8	6.3

Table 5.2 4σ detections for white noise + PS

.

the average detections obtained directly on the real image are $N_{det} = 4.10$. Therefore, for the *quadratic* method with $\epsilon = 8000$ the improvement in the number of detections is of the order of 26%. Regarding the gain going from real to wavelet space at the 5σ level, we find that for the case of the MHWopt, the average gain is $\simeq 1.6$ as compared with $\simeq 2$ for the *linear* case, whereas the *quadratic fusion* gives a gain $\simeq 4.3$ ($\epsilon = 5000$) and the same r as in the linear case.

We repeat the analysis detecting objects above 4σ. The results are shown in table 5.4.1. For $\epsilon = 2000$, N_{det} is 7.54, as compared with 5.67 obtained with $\epsilon = 25000$ in the 5σ, in both cases the ratio $r \simeq 0.1$. Finally, the gain at the *quadratic* level is higher than 5 at the 4σ level for the considered cases.

5.4.2 The 44 GHz Planck Channel

In this case, the images we generate present a much more complicated structure as compared with the white noise case. On top of the image with the point sources, we add four diffuse components. The first one is the so-called Cosmic Microwave Background radiation. The other three components are the main Galactic foregrounds. They include the thermal emission due to dust grains in the Galactic plane, synchrotron emission by relativistic electrons moving along the Galactic magnetic field and bremsstrahlung emission due to free electrons. In addition, we add instrumental noise according to Planck specifications. In this case, the average $< S/N > \approx 2.3$.

We do a similar analysis as in the previous subsection. We use the MHWF and the undecimated multiscale method to decompose the initial image into 12 subimages. We apply then the linear and *quadratic fusion* techniques to combine the subimages and use the output for detection. For comparison purposes we filter the input image with the Mexican hat wavelet at the optimal scale ($R_{opt} = 1.2$ in pixel units) as well and apply a detector on it. The detector is the usual 5σ or 4σ threshold.

In table 5.3 we show the average number of real detections and false alarms when detecting directly at the 5σ threshold both on the real image and on the linear and quadratic combination. Again we have explored different values of ϵ and show the most interesting ones, $\epsilon = 2000$, 5000 and 8000. We also include the results obtained with the MHWopt. In table 5.4 we show the average number of real detections and false alarms when detecting directly at the 4σ threshold and for the cases $\epsilon = 1000$, 5000 and 7000.

First, we remark that the average number of detected sources above 5σ in the original image is $\simeq 1$, as compared with 4 obtained in the white noise case. This shows the

5σ	*Real*	*MHW*	*Linear*	*Quadratic*		
ϵ	-	-	0	2000	5000	8000
N_{det}	0.970	3.070	3.490	3.890	4.380	4.740
N_f	0.001	0.001	0.002	0.004	0.008	0.035
$r(\%)$	0.10	0.03	0.05	0.1	0.2	0.7
$< G >$	1.0	2.2	2.3	4.7	6.1	7.1

Table 5.3 5σ detections for white noise + PS + CMB + foregrounds.

5σ	*Real*	*MHW*	*Linear*	*Quadratic*		
ϵ	-	-	0	1000	5000	7000
N_{det}	1.560	4.540	5.150	5.430	6.330	6.710
N_f	0.037	0.015	0.014	0.036	0.200	0.340
$r(\%)$	2.31	0.32	0.27	0.65	3.0	4.8
$< G >$	1.0	2.1	2.3	6.0	8.9	11.1

Table 5.4 4σ detections for white noise + PS + CMB + foregrounds.

importance of using filters to enhance the signal and reduce the noise, and for this particular case, to remove the diffuse components efficiently. Comparing the *linear* case with the MHWopt, the average number of detections are 3.49 for the first and 3.07 for the latter (improvement of $\simeq 12\%$). In both cases the ratio $r \simeq 0.05\%$.

If we compare the average detections for the MHWopt with the quadratic case with $\epsilon = 8000$, we see that the detections are 3.07 and 4.74, respectively, allowing a ratio $r < 1\%$. This is an improvement of the order of 35% in the number of detections. Regarding the gain going from real to wavelet space, we remark that at the 5σ level: in the MHWopt case, the average gain is $\simeq 2.2$ as compared with $\simeq 2.3$ for the *linear* case, whereas the *quadratic fusion* gives a gain $\simeq 4.7$ ($\epsilon = 2000$).

In the 4σ case, the average number of detections for the quadratic case with $\epsilon = 1000$ is 5.43, compared with the 5σ case, where we had 4.74 detections (for $\epsilon = 8000$) and similar ratio. Finally, the gain at the *quadratic* level is higher than 6 for all the considered values of ϵ at the 4σ level.

5.5 Conclusions

In this chapter we have presented a new method that combines images that contain localized sources in such a way that the output image has minimum variance and the image fusion gives at the position of the source an unbiased estimator of the amplitude. We studied the *linear* and *quadratic* fusion approach. We have tested these ideas in the context of compact source detection in astronomical data. To do this, we have done one thousand simulations for each of the two cases we want to consider. First, white noise plus point sources, and second, color noise plus point sources for the 44 GHz Planck satellite channel specifications. In both cases we have compared the average number of real detections and false alarms for the *linear* and *quadratic* case with those obtained with the Mexican hat wavelet at the optimal scale, the best studied tool in CMB science to detect point sources.

For the white noise case and 5σ threshold, if we compare the linear and MHWopt case on the one hand, we find that the improvement is of the order of 23%. On the other hand, if we compare the quadratic fusion and the MHWopt, the improvement is $\simeq 25\%$.

When we consider the case of realistic simulations for the 44 GHz Planck channel at 5σ, comparing the MHWopt with the *linear fusion*, the improvement of the latter is of the order of 12%. Furthermore, we find that using the *quadratic fusion* we detect $\simeq 35\%$ more real sources than with the MHWopt (with $r < 1\%$). Moreover, if we compare the quadratic fusion method with the results obtained when no filtering is done, we detect around four times more objects for the same ratio r.

We remark that the parameter ϵ that appears in the *quadratic fusion* can be easily obtained. The implementation of the method is very straightforward and the CPU necessary to test the method is very small, of the order of seconds for a 118x118 image. In future works we plan to test these techniques with other backgrounds as the ones found for higher frequency channels in the Planck satellite.